Mon. Not. R. Astron. Soc. **000**, 000–000 (0000) Printed 21 December 2006 (MN LATEX style file v2.2)

Searching for hidden Wolf-Rayet stars in the Galactic Plane – 15 new Wolf-Rayet stars

L. J. Hadfield[1⋆], S. D. Van Dyk[2], P. W. Morris[3], J. D. Smith[4], A. P. Marston[5] and D. E. Peterson[6]

[1] *Department of Physics and Astronomy, University of Sheffield, Sheffield, S3 7RH, UK*
[2] *Spitzer Science Center, IPAC, California Institute of Technology, M/C 220-6, Pasadena CA 91125, USA*
[3] *NASA Herschel Science Center, IPAC, California Institute of Technology, M/C 100-22, Pasadena CA 91125, USA*
[4] *Steward Observatory, University of Arizona, Tucson, AZ 87512, USA*
[5] *ESA/ESAC, Villafranca del Castillo, P.O Box Apdo. 50727, 28080 Madrid, Spain.*
[6] *University of Virginia, Department of Astronomy P.O. Box 400325, Charlottesville, VA 22904-4325, USA*

ABSTRACT

We report the discovery of fifteen previously unknown Wolf-Rayet (WR) stars found as part of an infrared broad-band study of candidate WR stars in the Galaxy. We have derived an empirically-based selection algorithm which has selected ∼5000 WR candidate stars located within the Galactic Plane drawn from the GLIMPSE (mid-infrared) and 2MASS (near-infrared) catalogues. Spectroscopic follow-up of 184 of these reveals eleven WN and four WC-type WR stars. Early WC subtypes are absent from our sample and none show evidence for circumstellar dust emission. Of the candidates which are not WR stars, ∼120 displayed hydrogen emission line features in their spectra. Spectral features suggest that the majority of these are in fact B supergiants/hypergiants, ∼40 of these are identified Be/B[e] candidates.

Here, we present the optical spectra for six of the newly-detected WR stars, and the near-infrared spectra for the remaining nine of our sample. With a WR yield rate of ∼7% and a massive star detection rate of ∼65%, initial results suggest that this method is one of the most successful means for locating evolved, massive stars in the Galaxy.

Key words: stars: Wolf-Rayet — Galaxy: stellar content

1 INTRODUCTION

Wolf-Rayet (WR) stars – the chemically evolved descendants of the most massive stars (i.e. $\geq 25\,M_{\odot}$) – possess intense stellar winds and so continually enrich their local environments. Although rare in number, high mass-loss rates during the WR stage means that they can completely dominate the energetics and chemical enrichment of their local interstellar medium (ISM). For example, WR stars comprise only 10% of the massive stellar content of NGC 3603, but they are responsible for 20% of the ionizing photons and ∼60% of the kinetic energy released into the ISM (Crowther & Dessart 1998). WR stars have also been suggested as possible precursors of core-collapse supernovae of types Ib and Ic and γ-ray bursts.

Our Galaxy provides an excellent laboratory for studying massive stars, as we can resolve objects on small scales and so hope to achieve sample completeness. However, to date ∼300 WR stars have been observed in our Galaxy (van der Hucht 2006), ∼75 of which have been reported in the last five years. With ∼1000–2500 WR stars expected to be located within the Milky Way (Shara et al. 1999; van der Hucht 2001), it is highly likely that a large number of WR stars are still waiting to be uncovered.

Previous WR surveys have utilised optical narrow-band interference filters tuned to the strong, characteristic λ4686 Å He II/C III emission feature. These have proved to be extremely successful, with the last large-scale optical survey reporting 31 new WR stars (Shara et al. 1999). However, the Galactic Plane contains large amounts of gas and dust, such that high extinction means that many WR stars may remain "hidden" from view. Even if optical surveys were to go as deep as V=25 mag, it is estimated that one-third of the Galaxy's WR population would still remain undetected (Shara et al. 1999). As a result one must turn to longer, infrared (IR) wavelengths in an attempt to reveal this "missing" population. IR surveys have generally followed a narrow-band imaging approach in order to detect WR stars.

⋆ E-mail: l.hadfield@sheffield.ac.uk

WR features are much weaker at near-IR wavelengths, but for locating WR stars in stellar clusters this method has proved to be very successful (Crowther et al. 2006). Unfortunately, for large scale surveys, especially those concentrated towards the Galactic Centre, the observed success rate is very low. Homeier et al. (2003) confirmed only 4 new WR stars found using IR narrow-band images. With a lack of suitable filters for large-scale survey instruments (e.g., WFCAM on UKIRT), such surveys require large amounts of telescope time and produce large amounts of data. With many known WR stars found to be isolated in the field, it would appear that a significant number of WR stars may still be waiting to be found.

Williams & Antonopoulou (1981) and Van Dyk et al. (2006a) have showed that it is possible to distinguish WR stars via their broad-band near-IR colours. A combination of continuum and line emission properties of WR stars distinguishes them from other stellar populations at IR wavelengths, but as Van Dyk et al. (2006a) have found, they are not so distinct that a criterion devised for candidate selection would lead to an acceptable (in terms of telescope time) predicted success rate. After confirming these suspicions in a pilot spectroscopic observing run, they incorporated *MSX* 8.0μm data to their colour selection in order to broaden the colour baseline. This resulted in the discovery of one new WR star suggesting that a combination of near- and mid-IR data can potentially provide a better discriminant for WR stars.

Taking this scheme one step further, we have developed broad-band, IR colour selection criteria which exploits 2MASS (near-IR) and the mid-IR *Spitzer* GLIMPSE (Galactic Legacy Infrared Mid-Plane Survey Extraordinaire, Benjamin et al. 2003) surveys[1]. GLIMPSE imaged the inner regions of the Milky Way within $\pm1^\circ$ of the Galactic Plane at 3.6, 4.5, 5.8 and 8.0 μm with a sensitivity and resolution that excellently matches that of 2MASS (for a more detailed description of the GLIMPSE project see Benjamin et al. 2003). Covering only 220 square degrees of the Galactic Plane, the merging of GLIMPSE and 2MASS colours excludes the possibility of an all plane survey, but well complements previous WR searches, allowing progress potentially to be made in the search for "hidden" WR stars in our Galaxy.

This paper presents the discovery of 15 new WR stars confirmed via either optical or near-IR spectroscopic follow-up observations. It complements a similar study conducted by Marston et al. (2006, in prep) who report the discovery of six new WR stars. This paper is structured as follows: Sections 2 and 3 briefly summarise the empirical colour selection algorithm used for target selection and information regarding spectroscopic follow-up observations. The newly discovered WR stars are presented in Section 4, where we consider spectral classification and provide reddening and distance estimates for each star. Although the primary goal of this survey was the detection of WR stars, we have identified a large number of emission-line objects. We briefly discuss the non-WR detections in Section 6. Finally, we summarise our results and draw conclusions in Section 7.

[1] GLIMPSE enhanced products are available at http://data.spitzer.caltech.edu/popular/glimpse/

2 CANDIDATE SELECTION

In the following section we present a brief outline of the selection criteria used to generate an initial candidate list.

At IR wavelengths WR stars exhibit free-free emission characteristic of a dense stellar wind (Wright & Barlow 1975). This emission is superimposed upon the stellar continuum such that WR stars exhibit a flatter spectral energy distribution relative to normal early-type stars. In a future paper we will describe in detail the mechanisms which drive the population of WR stars and subclasses to exhibit their near- to mid-IR colours, following the phenomenology described by Van Dyk et al. (2006b).

We have considered the positions of the observed colours of known Galactic WR stars in all possible mid- and near IR colour-colour combinations (i.e., GLIMPSE only, 2MASS only and GLIMPSE + 2MASS) to investigate if it is possible to distinguish WR stars via their broad-band IR colours. We find that the known WR stars are best distinguished in two possible colour-colour combinations.

(i) **Mid-IR colours:** Figure 1(a) shows the mid-IR colours for stars contained in a $1^\circ\times 1^\circ$ degree of the Galactic Plane centred on l=312° ($b\pm1^\circ$). Overplotted are the observed mid-IR colours of the known WR stars, which clearly separate from the general stellar locus. WR stars appear to exhibit a mid-IR excess, with colours [3.6] – [8.0] > 0.5 and [3.6] – [4.5] > 0.1. WN and WC stars appear to exhibit similar colours, such that mid-IR colours alone do not differentiate between WR subtypes.

(ii) **Mid + near-IR colours:** Galactic WR stars also appear to be distinguished in a combination of near and mid-IR colours. The 2005 "reliable" GLIMPSE catalogue was cross-matched with the 2MASS all-sky point source catalogue using a search radius of 1″ to create the colour sequence shown in Figure 1(b). As expected, the majority of the objects follow the reddening vector, while the WR stars clearly exhibit an 8.0μm excess. The WR stars appear to follow a separate, well-defined path relative to the reddening vector. Again WN and WC stars exhibit similar colours, however, WC stars with unresolved circumstellar dust shells have a tendency to display the largest 8.0 μm excess.

Using the positions of the known WR stars we have outlined two regions of colour space (as indicated in Fig 1) which define our WR candidates. Of the $\sim2\times10^7$ objects common to both to the GLIMPSE and 2MASS catalogues, ~100 000 were initially selected as candidate WR stars.

To reduce this number of candidates we have imposed additional selection criteria and restricted ourselves to only the most reliable sources, i.e., objects that are unblended, unconfused and of the highest photometric quality. This does, of course introduce a sample bias against highly crowded regions, i.e., stellar clusters. In addition to these "quality flags", we have applied a 2MASS only (J–H vs H–K_S) colour selection criterion using the WR near-IR colour relation reported by Van Dyk et al. (2006a). Additionally, assuming that optical WR surveys are complete to B=14 mag (Shara et al. 1999), the final selection criterion was to place a B>14 magnitude limit for all sources which have optical counterparts within a 3″ radius listed in the USNO-A2.0 catalogue.

Including all of the above restrictions the final number

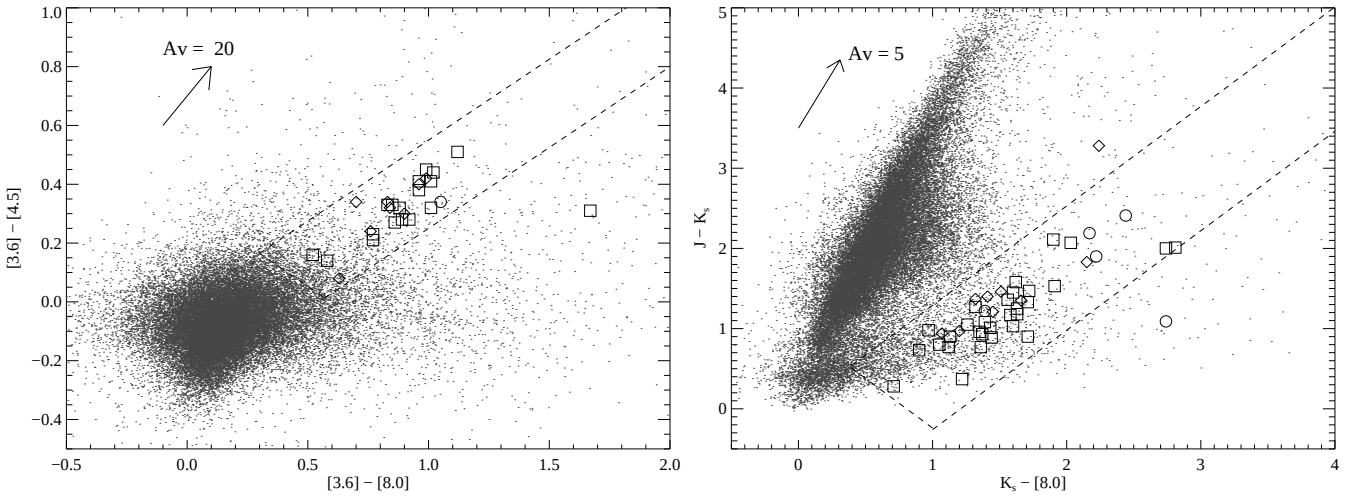

Figure 1. IR Colour-Colour diagrams for a 1°× 1° degree of the Galactic Plane centred on l=312° (b±1°). Previously reported Galactic WR stars (open symbols) clearly separate from the general stellar locus (points), and have been grouped into WN (squares), WC (diamonds) and WC9d (circles) stars. The dashed lines indicate the limits used over all GLIMPSE fields to select targets for spectroscopic follow-up. For a few cases, we find that their observed IR colours do not fall within the limits of our selection criteria. However, all of these are located in complex environments which would suggest unreliable photometry for these stars.

of WR candidates was reduced to ∼5700. Candidates were checked against known objects listed in the CDS SIMBAD database (http://simbad.u-strasbg.fr/), within a 10″ radius. Objects which already had spectroscopic classifications were excluded from our sample (∼1%). An additional ∼5% were listed as possible emission line objects or variable stars. The rest had no identification in SIMBAD.

In order to observe a representative sample for each longitude bin, targets were grouped by magnitude, and a subsample was selected at random from each magnitude bin. Objects that appeared to be extended in 2MASS or Digitized Sky Survey (DSS) images were excluded.

3 SPECTROSCOPIC OBSERVATIONS

The discovery of the fifteen new WR stars presented here is the result of four spectroscopic observing campaigns. Optically bright WR candidates in the Galactic latitude range of l=284°–350° were observed from the Cerro Tololo Inter-American Observatory (CTIO) on the nights of 2006 March 19–24. Near-IR spectroscopy of candidates within the GLIMPSE range l=0–65° was obtained from the Apache Point Observatory (APO) 2006 June 10–11 and the Infrared Telescope Facility (IRTF), Mauna Kea on 2006 August 8–9 and 11 and September 4–5. For classification purposes we have also observed a sample of known WR stars and transition stars. An observational log is presented in Table 1.

3.1 Optical Spectroscopy

Long-slit spectroscopic observations of 97 of our southern hemisphere candidates were obtained at the CTIO 4m-Blanco Telescope with the RCSpec spectrograph. Seeing conditions were ∼0.5″–1.0″, and all targets were observed at an airmass $\lesssim$1.6. Exposure times ranged between 300 s for our brighter targets (B∼15 mag), to 1800 s for the fainter objects (B∼19 mag). The data were obtained using the KPGL3 grating with a 1″ slit, resulting in a dispersion of ∼1.2 Å/pixel and resolution of 3.8 Å, as measured from comparison arc lines. The wavelength range of the final spectra was ∼4000–7500Å.

The data were cleaned of cosmic ray hits, de-biased and divided by a normalised flat field. Spectra were extracted using standard reduction routines within IRAF. Bad rows and pixels were masked assuming that they corresponded to ∼10σ outliers on flat-field images; any additional flaws were identified using the spectrum of the photometric standard star LTT 62648. Wavelength calibration arcs were taken at regular positions across the sky to allow for instrument flexure. Atmospheric absorption features have not been removed from the final spectra.

The majority of targets showed evidence of high extinction as the signal-to-noise ratio (S/N) of the spectra rapidly deteriorated at shorter wavelengths. The blue (∼4500Å) continuum S/N ranged from ∼1–30, versus ∼30–100 in the red (∼6800Å). Nevertheless, blue WR features were typically detected at the 25σ level.

3.2 Near-IR Spectroscopy

Near-IR spectroscopic follow-up observations of 87 candidate WR stars were acquired using the ARC 3.5-m with CorMASS (Cornell Massachusetts Slit Spectrograph, Wilson et al. 2001) and the IRTF 3.0-m with SpeX (Rayner et al. 2003).

CorMASS and SpeX are both near-IR cross-dispersed spectrographs. CorMASS is a low resolution detector and has a fixed slit width of 2.″0. SpeX is a medium resolution and was used in the short-wavelength cross-dispersed (SXD) mode with a 0.″8 and 0.″3 slit, resulting in R=750 and 2000, respectively. All near-IR observing modes resulted in a spectral coverage of 0.8–2.4μm.

Table 1. Observing Log

ID	Date	Observations	Slit ($''$)	R	Wavelength Coverage	Candidates Observed	WR Discoveries
(1)	2006 March 19–24	4.0m-Blanco/RCspec	1.0	900	3900–7500Å	97	6
(2)	2006 June 10–11	3.5m-ARC/CorMASS	2.0	300	0.8–2.4μm	26	2
(3)	2006 August 8–9, 11	3.0m-IRTF/SpeX	0.8	750	0.8–2.4μm	41	6
(4)	2006 September 4–5	3.0m-IRTF/SpeX	0.3	2000	0.8–2.4μm	20	1

In order to maximise the number of candidates observed, a limiting magnitude of K$\sim$10.5 and K$\sim$11.0 mag was imposed for Spex and CorMASS spectroscopy, respectively.

The Spex and CorMASS data were reduced using the Interactive Data Language reduction software tools Spextool v3.3 and Cormasstool v3.4 (Cushing et al. 2004). As the data were acquired using the standard "nod" technique, individual 2D frames were divided through by a normalised flat field before each pair was subtracted to produce a background-subtracted image; any residual background was subsequently removed during the extraction process. Spectra were extracted using an appropriate aperture radius, which for the majority of sources was $\sim 1''$.

Atmospheric features were removed from the final spectra by observing a selection of A0V standard stars following Vacca et al. (2003). The near-IR spectra of the nine of the bona-fide WR stars are shown in Figure A3.

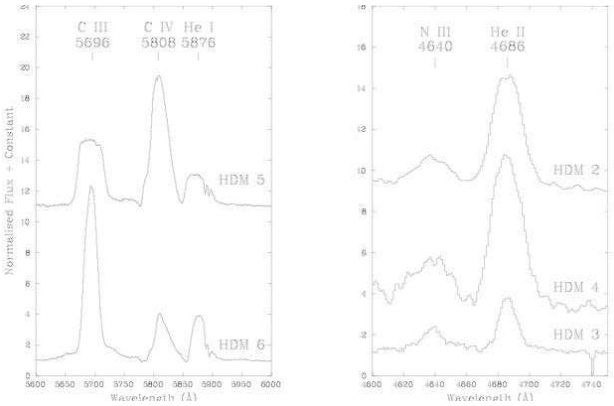

Figure 2. Optical CTIO/Rcspec spectra of the prominent yellow WC features (left) and blue WN (right) features.

4 RESULTS: 15 NEW WR STARS

Of the 184 candidates spectroscopically observed we have confirmed the discovery of 15 previously unknown WR stars. For brevity we have assigned a HDM nomenclature to these new discoveries. 2MASS designations and magnitudes of these new discoveries are presented in Table 2. K_S-band finding charts can be found in Appendix B.

4.1 Spectral Classification

Classification of WR stars via their optical spectra is relatively straightforward as schemes using optical line diagnostics are well defined (Smith et al. 1996; Crowther & Smith 1996). In the near-IR, classification is somewhat more difficult as there are no line diagnostics which uniquely distinguish all WR subtypes (Figer & McLean 1997; Crowther et al. 2006). Optical and near-IR classification will therefore be discussed separately.

4.1.1 Optical Classification

The reduced optical spectra (normalised to the continuum) are presented in Figure A1, grouped into WN and WC subtypes. Prominent WR emission features are identified. In order to classify the newly discovered WR stars, we have fit Gaussian line profiles to the prominent WR features. Measured equivalent widths and FWHM of the prominent optical WR features are presented in Table 3.

As Fig 2 shows, HDM 5 and 6 both display strong carbon features associated with late-type WC subtypes. Following the quantitative WC classification scheme of Crowther et al. (1998), refined from that of Smith et al. (1990), we assign WC7 and WC9 subtypes to HDM 5 and HDM 6, respectively.

Late-type WC stars have the potential of being surrounded by circumstellar dust shells which contribute thermal emission to the stellar continuum at mid-IR wavelengths, depending on dust temperature and density. Using optical spectroscopy it is not possible to directly confirm the presence of dust. However, both HDM 5 and 6 display near-IR colours consistent with non-dusty WC stars.

The remaining four WR spectra display He and N emission features indicative of WN stars. For this analysis we have adopted the classification scheme of Smith et al. (1996) and the observed He I λ5876 / He II λ5411 line ratios indicate a WN7 subtype for HDM 3, and WN6 for both HDM 2 and 4.

The spectrum of HDM 1 exhibits distinct differences to the other WN stars in our sample. The spectral features are notably narrower (FWHM$\sim$7Å) and lower excitation features are present. We compare the blue ($\lambda\lambda$4600–5000) and yellow ($\lambda\lambda$4600–5000Å) spectrum (normalised to the continuum) of HDM 1 with that of Galactic star NS4/WR105 (WN9) and LMC star Sk–66 40 (WN10) in Figure 3. The "blue WR bump" (He II, N II–III and C III) is clearly present, as are yellow N III, C III and Si III features. The spectral appearance of HDM 1 is remarkably similar to that of the comparison stars, and from that standpoint we classify HDM 1 as WN9/10. Spectral types WN9–10 are distinguished using the relative strengths of the blue N II–IV emission lines (Smith et al. 1996; Crowther & Smith 1997). Poor blue *S/N* prevents a classification based on this method for our object, so we have used the He II λ4686 vs. the He I λ5876 lines as a subtype indicator (Crowther & Smith 1997). This favours

Table 2. Data for the newly discovered Wolf-Rayet stars found by our survey. JHK_s magnitudes are taken from the 2MASS catalogue and mid-IR magnitudes correspond to values listed in the 2005 reliable GLIMPSE catalogue. Blue and red magnitudes are those listed in the 2MASS catalogue and are taken from the USNO-A2.0 Catalogue.

Star	2MASS Designation	l	b	B	R	J	H	K_s	[3.6]	[4.5]	[5.4]	[8.0]	Obs ID
HDM 1	11423766–6241193	295.13	–0.86	18.5	16.6	11.50	10.54	9.81	9.07	8.66	8.42	7.60	(1)
HDM 2	12065647–6238304	297.85	–0.21	17.8	15.3	11.55	10.82	10.22	9.56	9.19	8.99	8.59	(1)
HDM 3	12133878–6308580	298.68	–0.59	17.7	14.5	10.56	9.64	9.03	8.25	7.99	7.74	7.35	(1)
HDM 4	12461614–6257234	302.34	–0.09	19.6	16.5	12.18	11.22	10.56	9.81	9.43	9.21	8.27	(1)
HDM 5	13101207–6239065	305.08	+0.14	18.1	15.7	11.06	10.09	9.32	8.59	8.32	8.13	7.79	(1)
HDM 6	16113927–5205458	331.03	–0.50	18.3	15.3	10.16	9.25	8.46	7.86	7.48	7.36	6.89	(1)
HDM 7	18094505–2017103	10.23	–0.41	–	–	12.58	11.06	10.14	9.10	8.74	8.49	8.07	(3)
HDM 8	18131420–1753434	12.72	+0.02	19.2	15.2	9.62	8.60	9.94	7.32	6.87	6.71	6.34	(3)
HDM 9	18192219–1603123	15.04	–0.39	16.5	14.3	9.09	8.30	7.76	7.13	6.80	6.65	6.22	(3)
HDM 10	18250024–1033236	20.53	+0.98	–	–	12.21	11.24	10.61	9.74	9.33	9.03	8.67	(4)
HDM 11	18255310–1328324	18.05	–0.57	–	–	10.32	9.52	8.96	8.27	7.95	7.79	7.35	(3)
HDM 12	18400865–0329311	28.54	+0.92	–	–	11.77	10.86	10.30	9.54	9.28	8.99	8.64	(2)
HDM 13	18411070–0451270	27.44	+0.06	–	–	11.05	10.17	9.45	8.80	8.32	8.20	7.74	(3)
HDM 14	19081797+0829105	42.40	+0.15	–	–	10.59	9.47	8.71	8.09	7.60	7.38	6.97	(2)
HDM 15	19334401+1922475	54.91	–0.16	16.3	13.7	10.20	9.61	9.07	8.13	7.75	7.48	7.01	(3)

Table 3. Emission line equivalent widths (W_λ) and FWHM (both in Å) of prominent optical WR emission features. WR subtypes have been assigned using the classification schemes of Smith et al. (1996) and Crowther et al. (1998).

Star	N III/C III (4640/50)		He II (4686)		He II (5411)		C III (5696)		C IV (5808)		He II (5876)		H α (6560)		Spectral Type
	FWHM	W_λ	FWHM	W_λ	FWHM	W_λ	FWHM	W_λ	FWHM	W_λ	FWHM	W_λ	FWHM	W_λ	
HDM 1	9	10	9	10	–	–	7:	2:	–	–	7	30	9	85	WN9–10h
HDM 2	30	47	22	132	25	25	–	–	26	25	22	13	28	56	WN6o
HDM 3	20	17	14	33	11	5	–	–	weak	weak	15	7	24	57	WN7h
HDM 4	29	41	22	118	21	30	–	–	27	28	21	10	26	65	WN6o
HDM 5	25	343	25	119	25	30	37	83	42	212	31	289			WC7
HDM 6	19	107	21	42	12	10	21	68	24	292	22	67			WC9

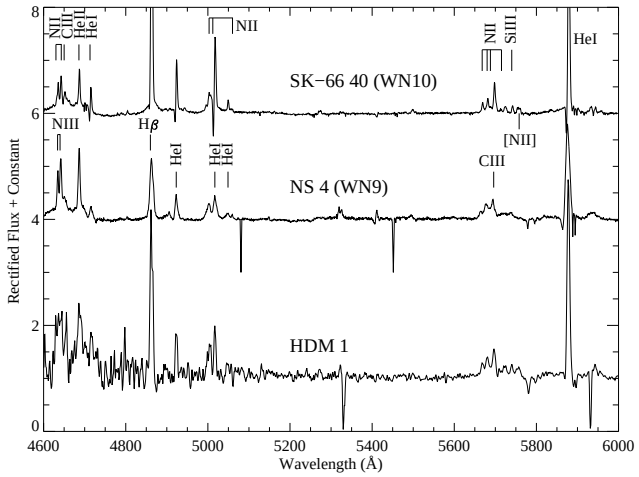

Figure 3. Comparison of HDM 1, NS4/WR105 (WN9) and LMC star Sk–66 40 (WN10). The spectra of NS4/WR105 and SK-66 40 are taken from Bohannan & Crowther (1999) and Crowther et al. (1995).

a WN9 subtype for HDM 1, but an accurate classification requires further observations.

WN stars can be further classified as weak or broad lined stars based on the FWHM of the He II spectral features. A star is considered to be broad lined if FWHM (He II 4686) $\geq$30Å and/or FWHM (He II 5411) $\geq$40Å (Smith et al. 1996). All of the WN stars for which optical spectroscopy is available are consistent with weak/narrow lined WN stars.

WR stars are normally hydrogen deficient objects, so the presence of hydrogen in WN stars has an important role from an evolutionary standpoint. A detailed abundance determination would, of course, require a quantitative spectral analysis, but it is possible to assess the presence of hydrogen using Pickering and Balmer lines at optical wavelengths.

Using blue He II / He II + Hβ line ratios, Smith et al. (1996) denote the presence of hydrogen with an additional o, (h), h, classification to signify no, weak or strong hydrogen. For our sample, poor S/N data prevents a reliable analysis of He II λ4541 and so we have qualitatively assessed our spectra using He II + Hβ (λ4860), He II+ Hα (λ6560) and He II (λ5411). Only for HDM 1 and 3 are the hydrogenic He II lines strong relative to He II λ5411, suggesting a WN9–10h and WN7h classification for these objects.

4.1.2 Near IR Classification

Recently, with reference to optical line diagnostics (i.e., helium and carbon lines), Crowther et al. (2006) presented

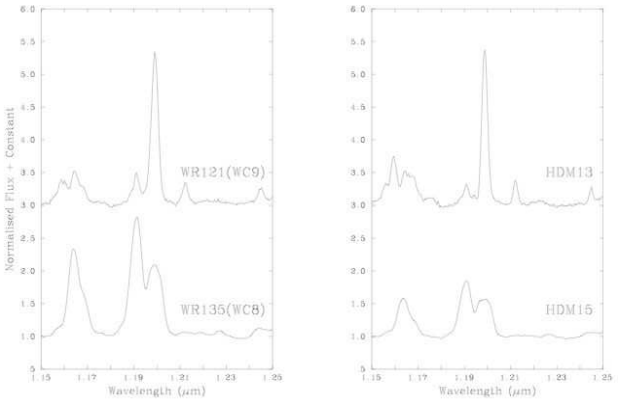

Figure 4. Spectral comparison of the near-IR C III / C IV morphology of WR 121 and WR 135 with HDM 13 and 15. All spectra were acquired with the IRTF and SpeX.

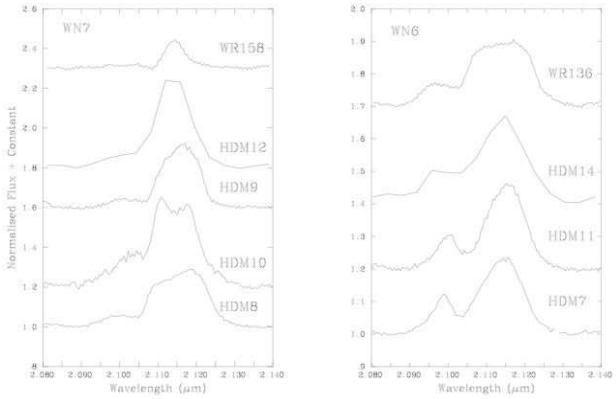

Figure 5. A spectral comparison of the near-IR N III / N V morphology of the newly discovered WN7 (left) and WN6 (right) stars with that of WR 158 (WN7) and WR 136 (WN6b).

a near-IR classification scheme which showed that these line diagnostics serve as reliable subtype discriminators. For stars earlier than WN6 or WC7, classification requires additional nitrogen and carbon diagnostics. Here, we have a adopted the classification scheme of Crowther et al. (2006) as well as making spectral comparisons with previously known WR stars. Line strengths of the prominent near-IR WR features are summarised in Table 4.

HDM 13 and 15 both display strong near-IR carbon features and from z and K-band C IV/C III line ratios we infer WC9 and WC8 subtypes for HDM 13 and 15. These classifications are confirmed in Figure 4, where we compare the C IV 1.19 and C III 1.20 μm features of the newly discovered WR spectra with those of well-classified WC stars.

The presence of circumstellar dust is easily inferred from near-IR spectra as the WR K-band spectral features are diluted by dust emission. Of the newly presented WC spectra, none show evidence of dust emission.

For HDM 7–12 and HDM 14 spectral features are consistent with nitrogen-rich WR stars. He II 1.012μm / He I 1.083μm and He II 2.189μm / Brγ line ratios suggest a WN7 subtype for HDM 8–10 and 12, whereas we infer a WN4–6 subtype for HDM 7, 11 and 14.

For WN4–6 stars, He line diagnostics do not provide a unique discriminator and the spectral type must be further refined using the 2.11 μm N III / N V morphology. For the stars presented here N III is strong relative to N V, and all have N line ratios consistent with a WN6 subtype (see Fig 5).

In the near-IR, WN stars are classified as broad-lined stars if the FWHM (He II 2.1885μm) $>$ 130 Å (Crowther et al. 2006). Using this criterion, HDM 8 and HDM 10 both qualify as being a broad-lined WN, such that we assign WN7b to these stars.

The presence of hydrogen can be assessed from the near-IR spectra using the He II 2.1889 μm / Brγ line ratios. Observed line ratios for the WN6 stars mimic those of the H-deficient WN6 stars in Westerlund 1 (Crowther et al. 2006), such that we strongly suspect that our WN6 stars are H-deficient. The same conclusions can be drawn for the narrow lined WN7 stars.

4.2 Extinction and Distance

WR photometry can be used to estimate the extinction and distance towards our stars, providing we have a calibration of intrinsic colours and absolute magnitudes. In principle, both visual and IR wavelengths can be used to derive reddenings for our sample, but with extinction at *JHK* wavelengths expected to be relatively insensitive to the line-of-sight we have chosen to assess the reddening and distances of our stars using their 2MASS JHK_S colours (Indebetouw et al. 2005).

Interstellar K-band absorption has been estimated by comparing the observed and subtype-dependent intrinsic J–K_S and H–K_S colours. Heliocentric distances have been derived using the mean value of A_{K_S}. The $A_{[\lambda]}/A_{K_S}$ ratios are taken from Indebetouw et al. (2005) and intrinsic WR photometric properties are those listed in Crowther et al. (2006). Intrinsic WR colours correspond to ESO/SOFI JHK_S filters whereas absolute magnitudes are based on 2MASS photometry. Since SOFI and 2MASS have comparable filter passbands, there should be negligible differences between SOFI and 2MASS intrinsic WR colours. Galactrocentric radii (R_G) have been calculated assuming $R_\odot = 8.5$ kpc.

Derived K-band extinction and distance estimates for our WR sample are summarised in Table 5. In general we find that $\overline{A_{K_S}}$ ~0.8–1 mag, except for HDM 7 where $\overline{A_{K_S}}$ is significantly larger. This higher extinction is supported by DSS images which shows no evidence of an optical counterpart. All of the other WR stars in our sample appear to have optical counterparts, even though for some optical magnitudes are not listed in the USNO-A2.0 catalogue.

For the majority of our stars, A_K^{J-K} and A_K^{H-K} are in good agreement (to within ~0.1 mag). WR stars are known to exhibit a wide range of intrinsic colours, and it is this scatter that leads to large uncertainties in our derived extinctions. The colour–subtype scatter of the stars which Crowther et al. (2006) used to estimate intrinsic WR colours lead to 10% uncertainties in derived extinctions.

For HDM 5, A_K^{J-K} and A_K^{H-K} differ by 0.4 mag, suggesting that our adopted WC7 intrinsic colours are unsuitable. If this star has intrinsic IR colours more consistent with those observed for WR68 (i.e., $[J-K]_o$=0.24, $[H-K]_o$=0.32, van der Hucht 2006), A_K^{J-K} and A_K^{H-K} would be consistent to within 0.2 mag, and $\overline{A_K}$ would in-

Table 4. Emission line equivalent widths (W_λ, in Å) of near-IR emission line diagnostics used to classify the new WR stars. WR subtypes have been assigned using the classification scheme of Crowther et al. (2006).* indicates that it was not possible to de-blend the spectral feature and values quoted refer to the strength of the whole feature.

Star	He II (1.012μm)	He I (1.083μm)	N V (2.110μm)	N III/He II (2.115μm)	He II+Brγ (2.165μm)	HeII (2.189μm)	Spectral Type
HDM 7	221	187	40	90	7	31	WN6o
HDM 8	132	338	10	45	59	62	WN7b
HDM 9	54	244	52	32	3	38	WN7o
HDM 10	230*	720*	9	65	87	77	WN7b
HDM 11	194	207	42	84	6	30	WN6o
HDM 12	69	350	58	28	5	49	WN7o
HDM 14	262	262	55	102	9	34	WN6o
	C III (0.971μm)	C II (0.990μm)	C IV (1.191μm)	C III (1.198μm)	C IV (2.076μm)	C III (2.110μm)	
HDM 13	95	70	11	73	9	78	WC9
HDM 15	363	19	51	42	270*	95	WC8

Table 5. Estimates of the extinction ($\overline{A_K}$) and distance (D) derived using 2MASS near-IR colours. Intrinsic colours and absolute K_S magnitudes are taken from Crowther et al. (2006). Galactrocentric radii (R_G) have been calculated assuming $R_\odot = 8.5$ kpc.

HDM	SpType	K_S	$A_{K_s}^{J-K}$	$A_{K_s}^{H-K}$	$\overline{A_K}$	M_{K_s}	D	R_G
1	WN9-10h	9.81	1.12	1.04	1.08	-5.92	8.5	9.1
2	WN6o	10.22	0.79	0.76	0.78	-4.41	5.9	7.8
3	WN7h	9.03	0.91	0.93	0.92	-5.92	6.4	7.8
4	WN6o	10.56	0.91	0.97	0.94	-4.41	6.4	7.4
5	WC7	9.32	0.36	0.75	0.55	-4.59	4.7	7.0
6	WC9	8.46	0.96	0.98	0.97	-6.30	5.7	4.5
7	WN6o	10.14	1.38	1.51	1.44	-4.41	4.2	4.5
8	WN7b	7.94	0.71	0.87	0.79	-4.77	2.4	6.2
9	WN7o	7.76	0.78	0.80	0.79	-5.92	3.8	5.0
10	WN7b	10.61	0.65	0.82	0.74	-4.77	8.5	3.0
11	WN6o	8.96	0.73	0.79	0.76	-4.41	3.3	5.4
12	WN7o	10.30	0.82	0.89	0.86	-5.92	11.8	6.0
13	WC9	9.45	0.84	0.91	0.87	-6.30	9.4	4.4
14	WN6o	8.71	1.09	1.13	1.11	-4.41	2.5	6.9
15	WC8	9.07	0.29	0.47	0.38	-4.65	4.7	7.0

crease from 0.55 to 0.90 mag. This increase in extinction would reduce our estimated distance from 4.7 kpc to 4.0 kpc.

Intrinsic absolute K_S-band magnitudes are also seen to display a large scatter, even when considering individual WR subtypes. With the observed spread in M_{K_S} being of the order of $\pm$0.5 mag (Crowther et al. 2006), and assuming that this dominates the uncertainty in our derived distances, we estimate that our heliocentric distances are correct to within $\sim$25%.

5 GALACTIC WR DISTRIBUTION

In order to investigate how the distribution of newly discovered WR stars compares with that of the previously known Galactic WR stars it is necessary to recompute distances to the WR stars listed in the VIIth Catalogue of WR stars, and its Annex (van der Hucht 2001, 2006) using the intrinsic near-IR colour/magnitude calibrations described in Section 4.2. For those WR stars which belong to stellar clusters or OB associations, we have adopted previously derived distances from the literature (see van der Hucht (2001); Crowther et al. (2006) and references therein). The only exception is for the highly obscured cluster SGR 1806–20, where our derived distance (based on a WN6 calibration) suggests a distance of $\sim$6 kpc rather than that of 15 kpc proposed by Eikenberry et al. (2004).

For binary members, extinction estimates have been made assuming that the WR star dominates the near-IR colours of the system. The absolute magnitude of the system has been calculated using the synthetic O-star photometry of Martins & Plez (2006). Binarity was only considered for cases where the companion star is well classified.

Estimating the extinction towards dusty WC stars using near-IR photometry is not straightforward since the associated circumstellar dust can exhibit a wide range of properties. At optical wavelengths the contribution of dust is negligible so that optically derived extinctions should, in principle, be more realistic than those estimated from IR colours. Therefore, solely for dusty WC stars, A_K has been estimated from optically derived extinctions listed in the VIIth Catalogue assuming that A_V=8.8A_K (Indebetouw et al. 2005). Distances were then derived adopting M_{K_S}=–8.5$\pm$1.5 mag (Crowther et al. 2006). Applying this calibration to WR95 yields a heliocentric distance of 3.9 kpc. With the large uncertainty associated with M_{K_S}, this consistent with that of 2.5 kpc inferred from its membership of Trumpler 27.

In Figure 6 we show the updated Galactic distribution of WR stars, as projected onto the Galactic Plane. We confirm conclusions of Conti & Vacca (1990), namely that the WR stars appear to trace the spiral structure of the Galaxy, with one spiral feature extending towards $l\sim280°$. Additionally, the Galactic WR distribution shows remarkable similarities to that of radio selected HII regions (Russeil 2003, their Fig 3).

The majority of the new WR stars are located between 4 kpc $\lesssim R_G \lesssim R_\odot$, the region where most of the previously known WR stars are observed to cluster. The exceptions are HDM 10, 12 and 13 which appear to be isolated from the bulk of the Galactic WR stars. This distribution suggests

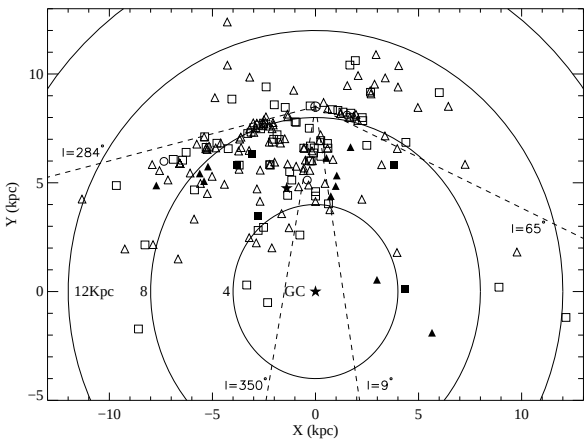

Figure 6. The Galactic WN (triangles), WC (squares) and WO (circles) distribution as projected onto the Galactic Plane. Open symbols correspond to previously catalogued WR stars (van der Hucht 2001, 2006) whereas filled symbols represent the new WR stars presented here. The Sun ($\odot$) corresponds to a Galactrocentric distance of 8.5 kpc and the symbol at the centre of the plot represents the Galactic Centre, Arches and Quintuplet clusters (N_{TOT}[WR]=60). The 24 WR stars located within Westerlund 1 are also represented by a star and have an assumed distance of 4.5 kpc. The dashed lines indicates the latitude coverage of the GLIMPSE survey.

that our survey has identified WR stars situated in more obscured regions of the inner Galaxy, rather than those which are more distant from the Sun.

Recalling from Section 3.2, arbitrary magnitudes limits of K_S ∼10.5 and K_S ∼11.0 mag were placed on IR spectroscopic observations to allow the maximum number of targets to be observed. This observational limit obviously influences the distribution of the newly discovered WR stars shown in Figure 6 and the maximum distance out to which we can detect WR stars is, of course, subtype dependant. For example, an early-type WR star (M_{K_S} ∼–4 mag) at a distance of 15 kpc would have a minimum apparent K_S magnitude of 12 mag, well below the limiting magnitude of any of our followup observations and the GLIMPSE [8.0μm] completeness limit of 9.5 mag.

Adopting an average K-band extinction of 0.86 mag (Table 5) and a limiting magnitude of K_S =10.5 mag, our observations are capable of identifying early and late-WN stars within ∼6.5 and 13.5 kpc of the Sun, respectively. Similarly for WC stars, observations of WC5–8 and WC9 subtypes are limited to within 7.5 and 12 kpc of the Sun, respectively.

If we were to extend our observations to cover the fainter targets in our sample, then it is possible that we could probe the WR population at larger distances. However, this may prove to be difficult as a combination of larger photometric uncertainties and crowding issues may significantly affect the reliability of our selection criteria, severely reducing the success rate of the survey.

It is well established that the absolute number and subtype distribution of a WR population is dependant on metallicity (Massey 2003). In the Milky Way, a slight metallicity gradient ($\Delta \log(\mathrm{O/H}) = -0.044 \pm 0.01 \mathrm{dex\,kpc^{-1}}$ [Esteban et al. (2005)]) is reflected by a preponderance of late-type WC and early-type WN stars at smaller galactrocentric distances.

Table 6. Galactic distribution of WR stars as a function of Galactocentric distance. log(O/H)+12 is quoted for R_G = 6.0, 8.5 and 10 kpc, assuming $\log(\mathrm{O/H})_\odot$+12=8.66 (Asplund et al. 2004) and a metallcity gradient of Esteban et al. (2005).

R_G	<7.0	7.0–10.0	>10
log(O/H)+12	∼8.8	8.66	∼8.5
N_{WN}	96	68	13
N_{WC}	81	41	6
N_{WO}	1	2	0
N_{WC}/N_{WN}	0.84	0.60	0.46
N_{WNE}/N_{WNL}	0.4	3	2
N_{WCE}/N_{WCL}	0.01	1	2

In Table 5 we list the number and subtype distribution of Galactic WR stars according to our near-IR derived distances. This shows that the number of WC stars relative to WN stars decreases with Galactocentric radius, confirming the earlier conclusions of Conti & Vacca (1990) and van der Hucht (2001). Using oxygen abundance as a proxy for metallicity, the early-to-late subtype distribution is seen to be extremely sensitive to metallicity, especially for WC stars. At Solar metallicity we count an equal number of WCE stars relative to WCL stars whereas at higher metallicity WCL stars significantly outnumber their early-type counterparts. At larger Galactic radii (lower metallicities) early-type stars dominate the WC population with a WCE/WCL ratio of ∼2. However, with only small number statistics, completeness is one important issue that must be considered when studying the WR distribution in the outer regions of the Milky Way. Similar conclusions are drawn for WN stars with late-type stars being more common at smaller galactic radii, however the range of observed ratios is much less extreme than that for WC stars. These results confirm previous conclusions drawn about the Galactic WR distribution (Conti & Vacca 1990; van der Hucht 2001) but highlight how sensitive WR populations are to the metal content of their environment.

Over the last two decades WR populations have been well sampled for a variety of metallicty environments (Massey 2003). N(WC)/N(WN) is observed to range from ∼0.1 in the metal-poor SMC (Z≈0.2$Z_\odot$), whilst N(WC)/N(WN)∼1 for M 83. For Solar metallicities, observations of the inner regions of M 33 suggest N(WC)/N(WN)∼0.7, very similar to that of N(WC)/N(WN)=0.6 observed for 7.0 kpc< R_G <10 kpc. For the metal-rich inner Milky Way, Z is equivalent to that of M 83. In M 83, N(WC)/N(WN)∼1 comparable to 0.84 obtained for R_G<7.0 kpc.

6 NON-WR DETECTIONS

In order to better refine our selection criteria, it is vital to gain an understanding of the objects that mimic the IR colours of WR stars. In this section we will briefly comment on the objects which satisfied our selection criteria, but turned out not to be WR stars.

From spectroscopic follow-up observations, ∼75% of spectra displayed emission features (c.f., 15% in Homeier et al. 2003). In addition to the 15 WR stars, we have identified one previously unreported planetary nebula and ∼120 (65% of the total sample) emission-line objects. Of the 50 spectra (15% of the total sample) which did not contain emission features, the majority displayed strong H absorption features consistent with mid- to late-type (A–G) dwarf stars.

For the majority (∼80 stars) of our emission-line objects, emission features consisted of leading H transition lines; Hα and Hβ in our optical sample and Pβ and Brγ in our IR sample.

In Figure 7 we show the rectified spectra of a representative sample of these objects observed with the CTIO/RCSpec. Hα is always present in emission, whereas Hβ is seen in emission or absorption. In addition to Hα and Hβ, the majority of objects display He I λ6678 absorption/emission. Helium and hydrogen features are characteristic of early-type stars, but the absence of He II λ5411 is consistent with these objects being early B supergiants/hypergiants. Sources which do not show He I λ6678 must be later-type stars, possibly late B or early A supergiants.

We have also identified a subset (∼40) of objects which display rich emission-line spectra, including H, He I and numerous lower-excitation metal lines, especially Fe II. Objects which display these emission-line features and near-IR excesses are usually classified as peculiar B[e] stars. A comparison of one these objects with that of the B[e] star HD 326823 is presented in Fig 7, clearly illustrating the similar spectral morphologies. Consequently, based solely from a spectral comparison standpoint, we identify these objects as Be/B[e] candidates.

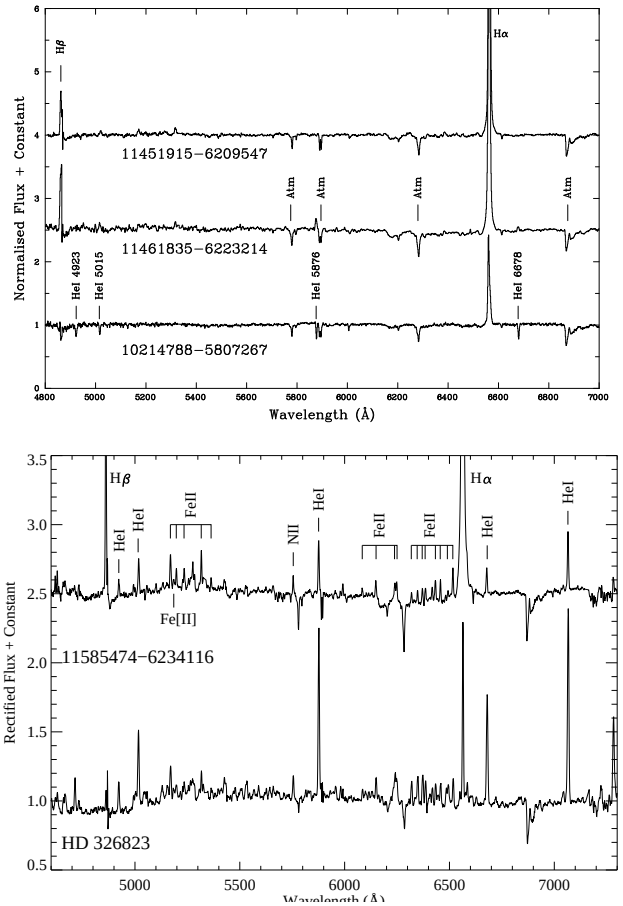

Figure 7. Non-WR detections. Top: A montage of CTIO/optical spectra of the Hα emission-line objects detected. Bottom: A spectral comparison of 2MASS source 11585474-6234116 with HD 326823 (B[e]). The spectra have been been vertically offset (by 1.5 continuum units) for clarity. Prominent emission features are marked.

7 DISCUSSION & CONCLUSIONS

Using a combination of near- and mid-IR colours we have identified candidate WR stars in the Galactic Plane using the observed colours of known Galactic WR stars as a "training set". Initial spectroscopic follow-up of 184 of our candidate WR stars has led to the discovery of eleven new WN and four new WC stars.

Up to now, WR searches have used narrowband K-band interference filters to search for emission line excesses, making them particularly insensitive to dusty WC stars. Here, we have detected both WN and WC stars, with none of the WC stars showing evidence for circumstellar dust.

The fifteen WR stars fall within $10°.2 < l < 331°.0$. For fourteen of these, we estimate that $R_G < R_\odot$ suggesting that this survey has been sampling WR stars located in nearby, highly obscured regions of the Galaxy. Since an all sky survey was not possible and follow-up spectroscopy was only capable of detecting the faintest WR subtypes to within ∼6.5 kpc, this survey is helping to complete the WR census within the Solar vicinity.

Many recent WR surveys have concentrated on finding WR stars in massive stellar clusters and with 30% of the Galactic WR stars being contained with four clusters (van der Hucht 2006), such searches are very worthwhile. Interestingly however, eight of the nine WR stars detected in recent photometric surveys (Hopewell et al. 2005; Homeier et al. 2003) and the fifteen WR stars presented here are located in relatively isolated regions. Continually finding WR stars in isolation raises many questions as to how they arrive there, are they runaway stars expelled from clusters by supernovae events or binary/close interactions, have their native clusters simply dispersed or do some massive stars actually form in isolation? Of course, with only small number statistics we cannot attempt to address such issues here, but it does highlight the importance of sample completeness and that searches for WR stars in the Galactic Plane are extremely worthwhile.

In addition to WR stars, we have identified one new planetary nebula and ∼120 H emitting sources within the Galaxy, most of which we believe to be massive OB supergiants/hypergiants. With a WR yield rate of ∼7%, and an massive star detection rate of ∼65%, our initial findings have proved that this survey is one of the most successful searches for evolved massive stars in the Galaxy. However, since GLIMPSE is restricted to $>\pm10°$ from the Galctic center, it is not possible that we will find all of the missing WR stars, but will, in fact, complement other ongoing WR searches.

Our survey has revealed that using a combination of 2MASS and GLIMPSE data it is possible to locate WR stars which had remained hidden from view behind copious amounts of dust. Assuming that subsequent follow-up observations of our remaining candidates achieves the same success rate, we have the possibility of increasing the known Galactic WR population twofold.

ACKNOWLEDGEMENTS

We wish to thank Michael Skrutskie and Michael Cushing for helping to acquire and reduce some of the spectra presented here and Bobby Bus for his invaluable assistance in showing us how operate SpeX. We also thank Paul Crowther for numerous, interesting discussions regarding our spectra.

Some of the data presented here was acquired as a visiting astronomer at the Infrared Telescope Facility, which is operated by the University of Hawaii under Cooperative Agreement no. NCC 5-538 with the National Aeronautics and Space Administration, Science Mission Directorate, Planetary Astronomy Program.

This work is part of a *Spitzer* Cycle-2 archive programme funded by JPL/Caltech and is part based on archival data taken by the *Spitzer* Space Telescope. This research has made use of the NASA/ IPAC Infrared Science Archive (IRSA). *Spitzer* and IRSA are operated by the Jet Propulsion Laboratory, California Institute of Technology under contract with NASA.

REFERENCES

Asplund M., Grevesse N., Sauval A., Allende Prieto C., Kiselman D., 2004, A&A, 417, 751
Benjamin R. A., Churchwell E., Babler B. L., et al. 2003, PASP, 115, 953
Bohannan B., Crowther P. A., 1999, AJ, 511, 374
Conti P., Vacca W. D., 1990, AJ, 100, 2
Crowther P. A., De Marco O., Barlow M. J., 1998, MNRAS, 296, 367
Crowther P. A., Dessart L., 1998, MNRAS, 296, 622
Crowther P. A., Hadfield L. J., Clark J. S., Negueruela I., Vacca W. D., 2006, MNRAS, 372, 1407
Crowther P. A., Hillier D. J., Smith L. J., 1995, A&A, 293, 172
Crowther P. A., Smith L. J., 1996, A&A, 305, 541
Crowther P. A., Smith L. J., 1997, A&A, 320, 500
Cushing M. C., Vacca W. D., Rayner J. T., 2004, PASP, 116, 362
Eikenberry S., Matthews K., LaVine J., et al. 2004, ApJ, 616, 506
Esteban C., Garci'a-Rojas J., Peimbert M., et al. 2005, ApJ, 618, 95
Figer D. F., McLean I. S., 1997, ApJ, 486, 420
Homeier N. L., Blum R. D., Pasquali A., Conti P. S., Damineli A., 2003, A&A, 408, 153
Hopewell E. C., Barlow M. J., Drew J. E., et al 2005, MNRAS, 252, 681
Indebetouw R., Mathis J. S., et al. 2005, ApJ, 619, 931
Marston A. P., Hadfield L. J., Van Dyk S. D., Morris P. W., Smith J. D., 2006, in prep
Martins F., Plez B., 2006, A&A, 457, 637
Massey P., 2003, ARA&A, 41, 15
Rayner J. T., Onaka P. M., Cushing M. C., Vacca W. D., 2003, PASP, 115, 362
Russeil D., 2003, A&A, 397, 133
Shara M. M., Moffat A. J., Smith L. F., Niemela V. S., Potter M., Lamontagne R. K. L., 1999, AJ, 118, 390
Smith L. F., Shara M. M., Moffat A. J., 1990, ApJ, 348, 471
Smith L. F., Shara M. M., Moffat A. J., 1996, MNRAS, 281, 229
Vacca W., Cushing M. C., Rayner J. T., 2003, PASP, 115, 389
van der Hucht K. A., 2001, New Ast. Rev., 45, 135
van der Hucht K. A., 2006, A&A, p. Accepted
Van Dyk S. D., Morris P. W., Smith J. D., 2006a, AJ, in review
Van Dyk S. D., Morris P. W., Smith J. D., 2006b, AJ, in prep
Williams P. M., Antonopoulou E., 1981, MNRAS, 196, 915
Wilson J. C., Skrutskie M. F., Colonno M. R., Enos A. T., Smith J. D., Henderson C. P., Gizis J. E., Monet D. G., Houck J. R., 2001, PASP, 113
Wright A. E., Barlow M. J., 1975, MNRAS, 170, 41

APPENDIX A: NEW WR SPECTRA

APPENDIX B: FINDING CHARTS

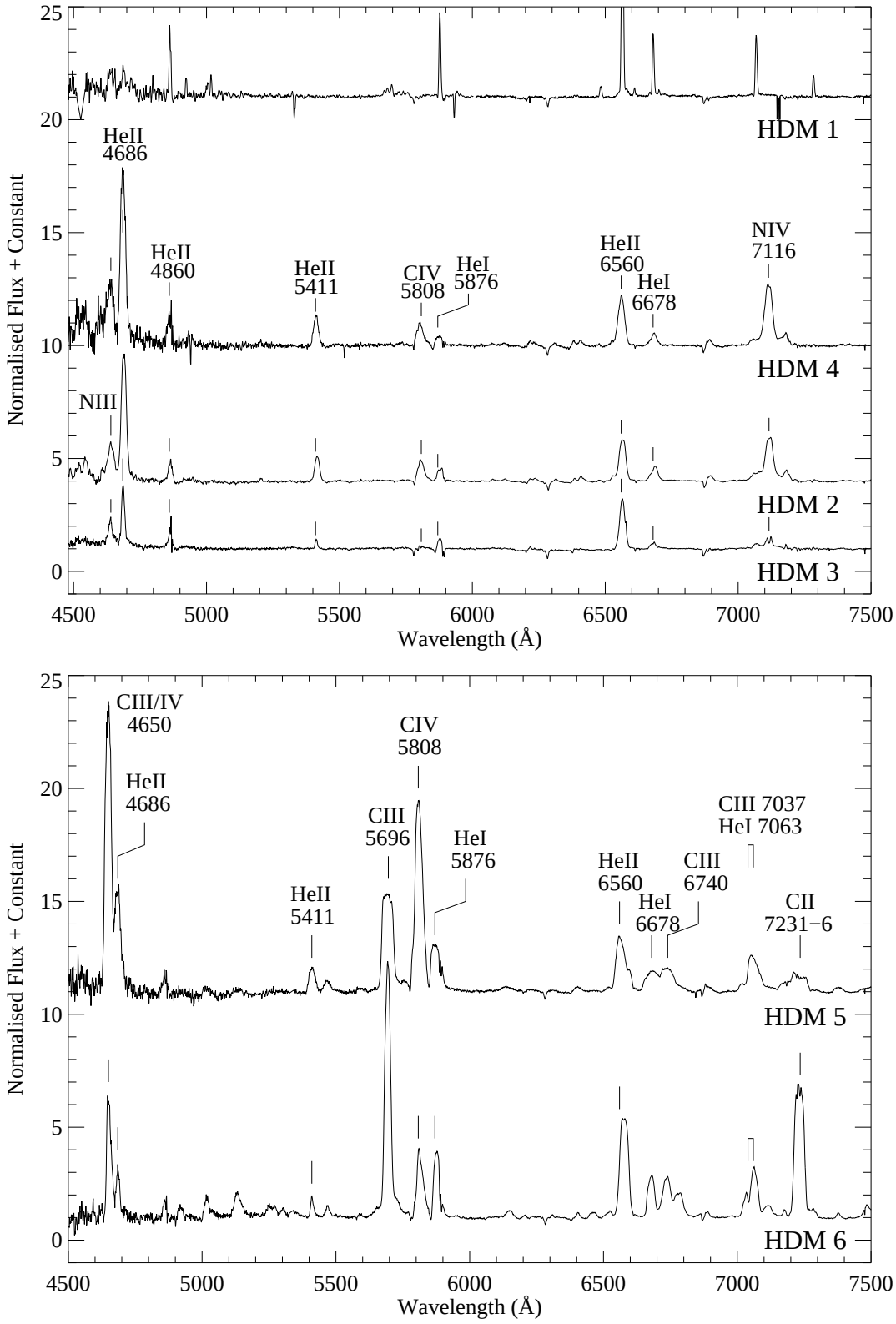

Figure A1. Optical CTIO/RCSpec data for six of the newly discovered WR stars. WN stars are given in the top panel and WC star are presented in the bottom panel.

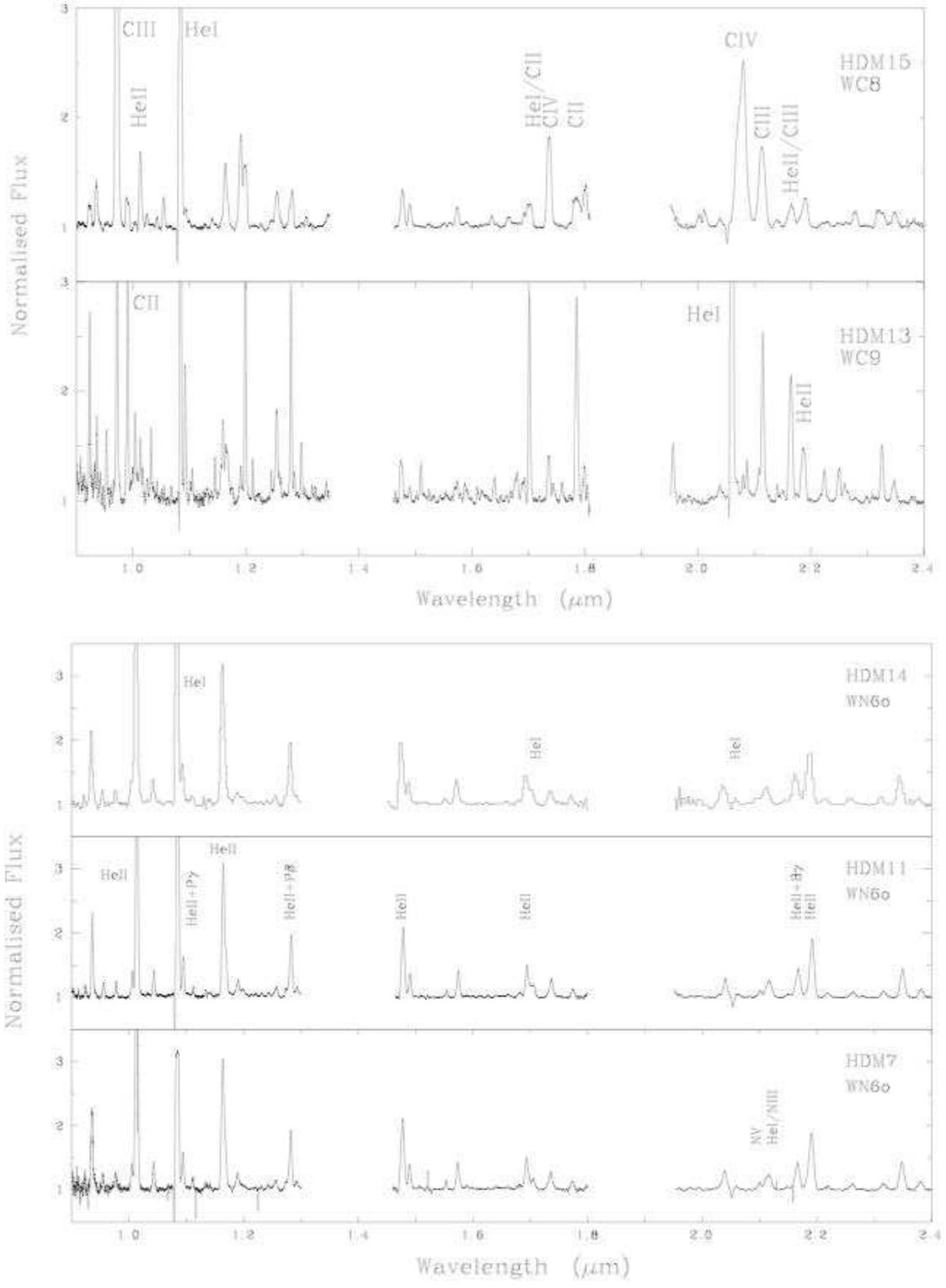

Figure A2. Near-IR spectra of five of the newly confirmed Galactic WR stars. WC stars are shown in the top panel and WN stars are bottom panel. The spectra were acquired using IRTF/SpeX, except for HDM 14 which was observed with APO/CorMASS.

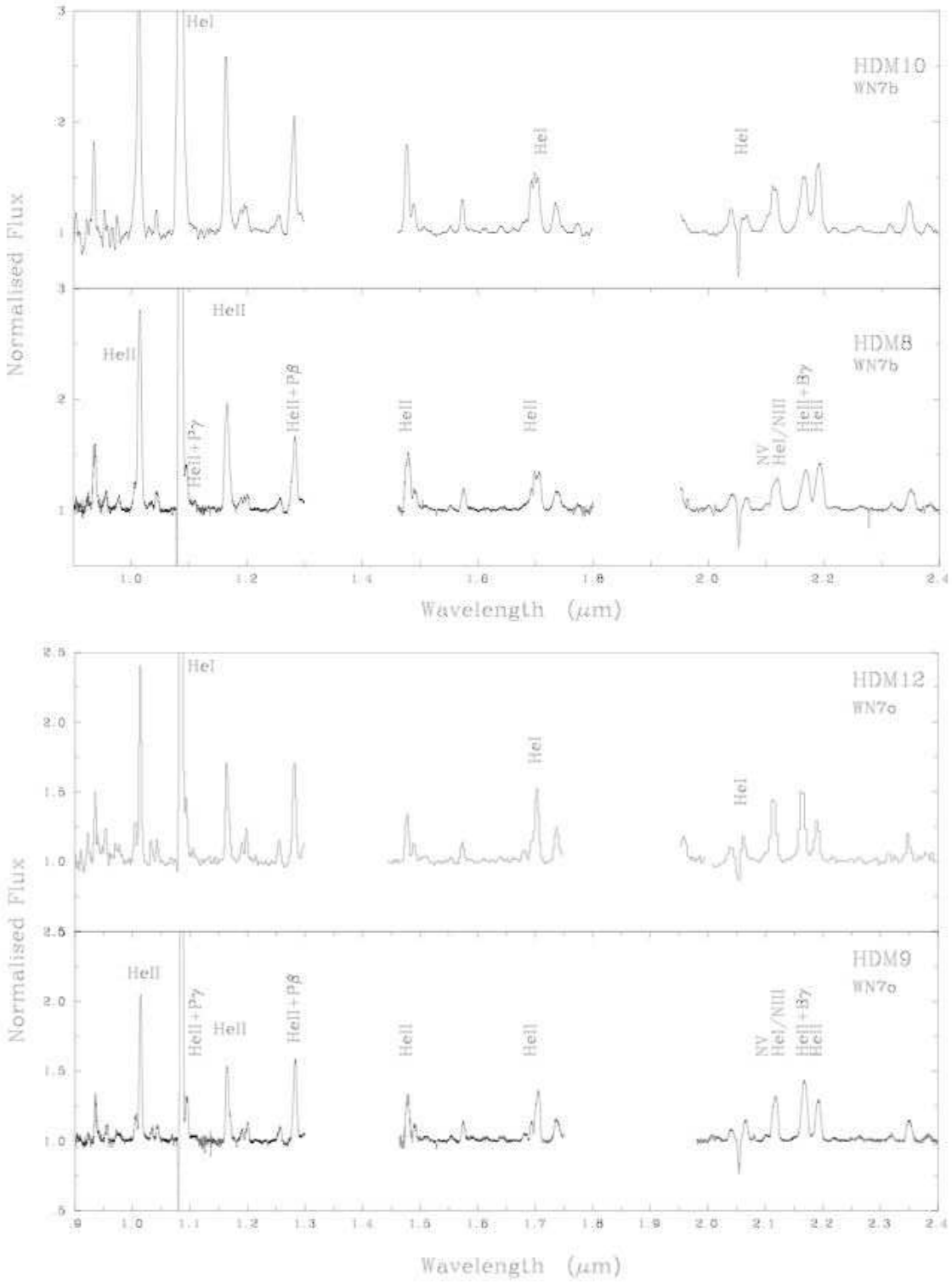

Figure A3. Near-IR spectra of the four newly confirmed WN7 stars. Spectra have been grouped into broad (top panel) and narrow-lined (bottom panel) stars. The spectra were acquired using IRTF/SpeX, except for HDM 12 which was observed with APO/CorMASS.

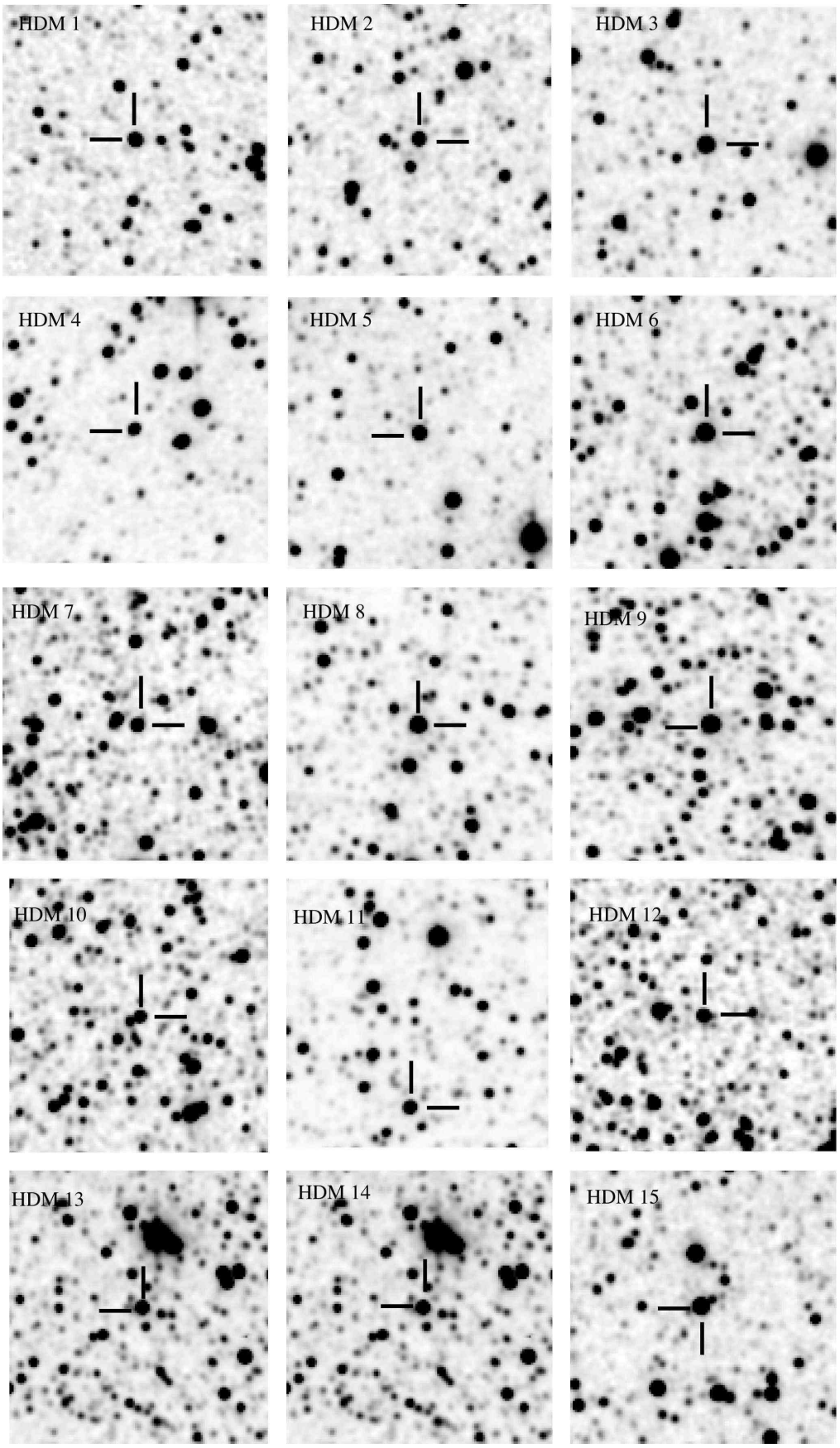

Figure B1. $2 \times 2'$ 2MASS K_S finding charts for the newly discovered WR stars. North is up and east is to the left on all images.